Synergistic Effects of Wear and Corrosion for Al_2O_3 Particulate–Reinforced 6061 Aluminum Matrix Composites

C.-K. FANG, C.C. HUANG, and T.H. CHUANG

Wear corrosion of alumina particulate–reinforced 6061 aluminum matrix composites in a 3.5 wt pct NaCl solution with a revised block-on-ring wear tester has been investigated. The studies involved the effects of applied load, rotational speed, and environments (dry air and 3.5 pct NaCl solution) on the wear rates of materials. Also various specimens with Al_2O_3 volume fractions of 0, 10, 15, and 20 pct were employed in this work. Electrochemical measurements and electron micrographic observations were conducted to clarify the micromechanisms of wear corrosion in such metal matrix composites. Experimental results indicated that the wear rate of monolithic 6061 Al in either dry wear or wear corrosion was reduced by adding alumina reinforcements. However, the effect of volume fraction on wear rate is only minor in dry wear, while it is significant in the case of wear corrosion. Wear-corrosion tests also showed that the corrosion potential shifted to the active side and the current density for an applied potential increased with the decrease of Al_2O_3 volume fraction in the materials and the increase in applied load and rotational speed. Although the incorporation of reinforcement in these aluminum matrix composites was deterimental to their corrosion resistance, the influence on wear corrosion was favorable.

I. INTRODUCTION

BECAUSE of the demands for high specific strength (strength-to-weight ratio) and specific stiffness, good high temperature capabilities and wear resistance in many engineering applications, metal-matrix composites (MMCs) have engendered extensive interest from industrial and academic researchers. The manufacturing processes of fiber-, whisker-, and particulate-reinforced MMCs have been well developed.[1] Because of the reduction in fabrication cost, the applications of MMCs have been widely extended to light weight bearing sleeves, calipers, automobile parts (brake rotors, drive shafts, connecting rods, piston rings, and cylinder liners), sporting goods, aerospace components, tanks (wheels, speed brakes, and track shoes), and other industrial applications. Among the three types of MMCs, particulate-reinforced MMCs are promising because of their isotropic material properties and low cost; additionally, they can be formed using conventional metal processing techniques.

It is well known that wear resistance is significantly improved if the proper amount of reinforcement particles is added to the matrix.[2,3] However, the corrosion of the matrix can be increased due to the incorporation of reinforcements. Lore and Wolf[4] investigated the corrosion of SiC-reinforced 2024, 6061, and 7075 aluminum alloy–based MMCs. They found that the increase in corrosion due to the reinforcement phase was the most significant for 6061 Al matrix compared to the other matrices. The corrosion behavior of Al-based MMCs has been extensively studied.[5–11] A review of corrosion studies on aluminum MMCs based on silicon carbide, graphite, alumina, and boron reinforcements can be found in Turnbull's[12] review article. In general, the reinforcement may introduce imperfections in the surface oxide on the matrix surface, and preferential attack occurs due to galvanic couples, active reaction products, intermetallic particles, microvoids, and microcrevices at reinforcement/matrix interfaces. Clustered areas of particles may also enhance corrosion attack.[13] For alumina fiber–reinforced aluminum MMCs, no evidence of galvanic corrosion between Al_2O_3 and aluminum was reported,[12] while interfacial corrosion was observed. The preceding articles concentrated mainly on fiber-, whisker-, or SiC_p-reinforced MMCs, while research on the corrosion behavior of alumina particulate–reinforced MMCs was rather limited.

Although wear properties and corrosion behavior have been widely studied for engineering materials, published literature dealing with wear corrosion is rather limited. The interaction of wear and corrosion is, however, crucial in engineering applications in the cases where corrosion is jointly responsible for the wear of metallic components, *e.g.*, chemical pumps, piston rings, cylinder walls, and mechanical seals, and the components in marine structures. In many cases, the wear rate in solutions is usually larger than that due to dry wear.[14,15] Because of the combined action of mechanical and electrochemical mechanisms, the volume loss due to the synergistic effect of abrasion corrosion often exceeds the sum of the separate abrasive and corrosive wear losses.[16]

Wear may result in the elevation of surface temperature, surface activation, and the removal of the oxide film or passive film and thus may accelerate oxidation or corrosion. On the other hand, the effect of corrosion on wear can be positive or negative, depending on the composition and hardness of the corrosion products. Corrosion may accelerate the wear damage through plowing by hard oxides. On the contrary, the formation of a film due to corrosion can

C.-K. FANG, Associate Professor, is with the Department of Mechanical Engineering, China Institute of Technology and Commerce, Taipei, Taiwan 11522, Republic of China. C.C. HUANG, Process Engineer, is with the Taiwan Semiconductor Manufacturing Company Ltd., Hsin-Chu, Taiwan, Republic of China. T.H. CHUANG, Professor, is with the Institute of Materials Science and Engineering, National Taiwan University, Taipei, Taiwan 106, Republic of China.

Manuscript submitted May 19, 1998.

impede adhesion and confer some degree of self-lubrication, resulting in reduced wear damage and coefficient of friction. Literature review on the study of wear-corrosion synergism can be found in Watson *et al.*[17] The quoted articles concentrated primarily on ferrous alloys, while the published literature on wear corrosion of MMCs is rather limited.[18]

Because of the reinforcement phase in the matrix, the mechanism of wear corrosion in MMCs is considerably complicated. For instance, wear resistance is significantly affected by the strength of reinforcement-matrix interfaces, while the interfaces between reinforcements and matrix may result in localized corrosion. Studies on sliding wear corrosion in MMCs are scarce in the literature, so the results from studies of a similar reaction, solid particle erosion corrosion, were reviewed. Using acid-sand media, Ji and Tang[19] studied the erosion-corrosion behavior of MMCs composed of WC particles and a chromium-alloyed matrix. They found that the compactness of WC particles in MMCs contributed to erosion-corrosion resistance in strong acid-sand media. However, such a trend did not exist in a water-sand medium. Using a rotating sample method, Saxena *et al.*[20] performed erosion-corrosion tests of an alumina fiber–reinforced aluminum alloy in 3 pct NaCl solution with sand particles. It was found that the composite suffered from more material loss than the monolithic alloy. The weight loss in the erosion-corrosion test was significantly higher than that in the immersion test. The erosion corrosion of particulate-reinforced aluminum MMCs was studied by Bester and Ball.[21] The addition of ceramic particles to the matrix alloys was found to have a detrimental effect on the slurry erosion resistance. Sliding wear corrosion was investigated by Yu *et al.*[18] on SiC whisker- and particulate-reinforced 6061 aluminum alloy composites. The effect of volume fractions of the reinforcement was not clear because only two volume fractions were studied in their article.

In the present article, the synergistic effects of wear and corrosion in alumina particulate–reinforced 6061 aluminum alloy composites with different volume fractions of reinforcement have been studied. The influence of corrosion on wear and that of wear on corrosion are studied. The results are compared with those in dry wear. The effect of volume fraction of reinforcement on wear corrosion is investigated as well.

II. EXPERIMENTAL PROCEDURE

A. *Specimen Preparation*

Monolithic 6061 aluminum alloy and Al_2O_3 particulate–reinforced 6061 aluminum alloy composites were used in the present work. Different volume fractions of the reinforcement in the Al_2O_3/Al were prepared, *viz.* 0, 10, 15 and 20 vol pct, denoted as 6061 Al, 10-Al_2O_3/Al, 15-Al_2O_3/Al, and 20-Al_2O_3/Al hereafter in the text. Table I gives the chemical compositions of the Al matrix in the test materials. The size of the Al_2O_3 particulates ranges from 10 to 30 μm in diameter. The as-cast materials in billet form were hot extruded into bars of 22 mm in diameter. The specimens for wear tests were cut from the bars and solution treated at 530 °C for 2 hours, and then quenched in cold water. Although it was recommended by Saigal and Leisk[22] that the alumina-reinforced aluminum 6061 alloy composites be solution treated for 6 hours for higher strength, the standard 2-hour solution treatment was used so that the results would be comparable with those of other reseachers. They were subsequently peak aged to a T6 condition (160 °C for 18 hours), and the hardnesses were tested. Since the volume fraction and spatial distribution of second phases may have a significant effect on the wear-corrosion behavior, the micrographs of the samples prior to testing were examined, as illustrated in Figure 1. Although the particles are aggregated in a nonuniform way, the distribution of aggregates looks uniform. Table II shows the physical properties of the materials. It was observed that the bulk hardnesses (HRB) and specific gravities of the composites increased with the increase of volume fraction of the Al_2O_3 reinforcement.

Table I. Chemical Compositions of the Monolithic 6061 Al-Alloy and the Aluminum Matrix of Various MMCs in This Study

	Elements (Wt Pct)								
Materials	Si	Fe	Cu	Mn	Mg	Cr	Zn	Ti	Al
6061 Al	0.43	0.31	0.31	0.05	0.94	0.13	0.20	0.03	bal
10-Al_2O_3/Al	0.57	0.04	0.24	0.01	1.05	0.15	0.04	0.02	bal
15-Al_2O_3/Al	0.48	0.05	0.22	0.01	0.90	0.14	0.05	0.01	bal
20-Al_2O_3/Al	0.69	0.04	0.20	0.01	1.00	0.15	0.05	0.01	bal

B. *Wear Tests*

Using a block-on-ring wear apparatus, as shown in Figure 2, dry wear tests in laboratory air and corrosive-wear tests in 3.5 wt pct NaCl aqueous solution open to air were performed. The solution was prepared from a mixture of reagent grade NaCl and distilled water. The wear pair made of sintered Al_2O_3 with dimensions $21 \times 21 \times 21$ mm^3, Hv $= 1460 \pm 20$, and a surface roughness of 1.0 μm was installed in a fixture, through which a load was applied to a ring-shaped specimen. The wear pair was insulated to avoid any influence on the electrochemical data of wear specimens. The ring-shaped wear specimens (20, 12.7, and 8 mm in outer diameter, inner diameter, and length, respectively) were formed mechanically from the extruded bars and finally polished with emery paper in discrete steps down to a 1000 grade finish. They were then degreased with acetone, washed in distilled water, and dried with hot air. The wear tests were conducted at loads of 5, 10, 15, and 20 N for 1 hour at rotational speeds of 100, 300, and 500 rpm. After testing, the specimens were ultrasonically cleaned with acetone and dried with hot air. The specimens were weighed before and after tests *via* an electronic balance with an accuracy of 0.1 mg. The wear rate, defined as the ratio of the weight loss (due to wear and corrosion) to the sliding distance, was computed for each specimen.

The surface morphologies of the specimens after testing were examined by scanning electron microscopy (SEM). Since the hardness of the wear pair (Al_2O_3 block) was far higher than that of the specimens and its wear volume was negligibly small, the wear properties of the wear pair were not considered in the present study.

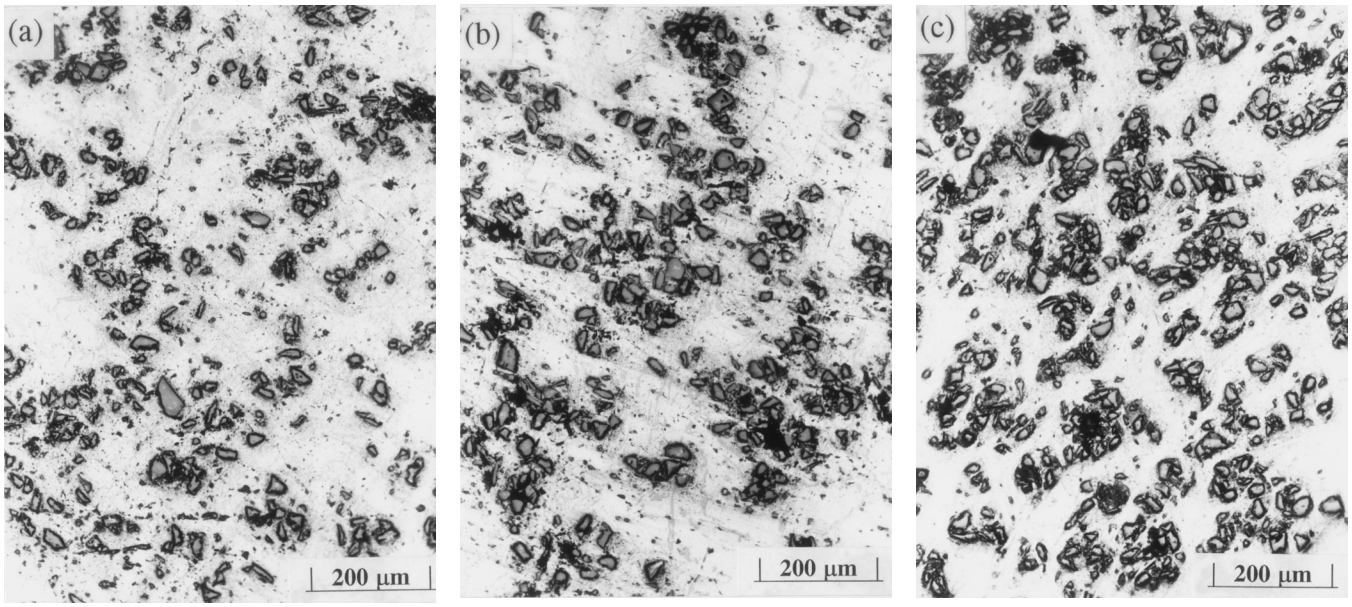

Fig. 1—Micrographs of the samples with different volume fractions of reinforcements: (*a*) 10 pct, (*b*) 15 pct, and (*c*) 20 pct.

Table II. Hardnesses and Specific Gravities of the Materials Heat Treated to the T6 Condition

Material	Hardness (HRB)	Specific Gravity (g/cm^3)
6061 Al	66.2	2.680
10-Al_2O_3/Al	69.7	2.771
15-Al_2O_3/Al	74.5	2.855
20-Al_2O_3/Al	76.1	2.899

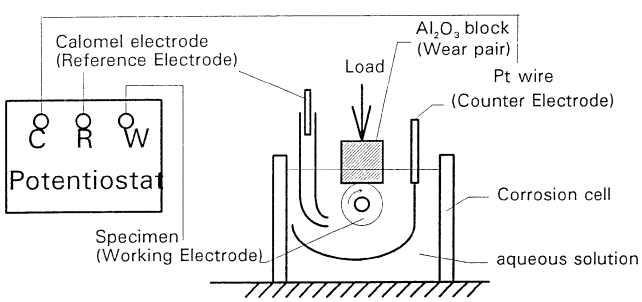

Fig. 2—The schematic diagram of the wear tester

C. *Electrochemical Measurements*

To investigate the effects of wear on corrosion, electrochemical behavior during corrosive wear in 3.5 wt pct NaCl aqueous solution open to air was analyzed using a potentiostat. In a three-electrode system, the specimen served as a working electrode, with a platinum wire encircling the specimen as a counterelectrode. A saturated calomel electrode (SCE) was used as a reference electrode. The open circuit potentials of specimens were measured prior to the polarization test. The potentiostatic anodic polarization curves were obtained by applying potential ranging from the open circuit potential to 0.5 V (SCE) at intervals of 0.1 V. At each applied potential, the wear lasted 2 to 4 minutes until the corrosion current became stable.

For comparison, potentiodynamic polarization curves were also generated in corrosion (without wear). In order to remove the oxidation film, a potential of −1.5 V (SCE) was applied to the working electrode for 5 minutes prior to the beginning of the experiment. The potential scan rate was 1 mV/s.

III. RESULTS AND DISCUSSION

A. *The Effect of Corrosion on Wear Properties*

In this section, the wear rates in dry wear and corrosive wear were studied for different applied loads at different rotational speeds, as presented in Figures 3 and 4. The solid lines show the results for dry wear in ambient air, while the dashed lines represent those for wear corrosion in 3.5 pct NaCl aqueous solution.

Figure 3 shows the effect of applied load on the wear rate in both environments. The results for different rotational speeds, *viz.* 100, 300, and 500 rpm, are illustrated in Figures 3(a) through (c), respectively. The wear rate is elevated monotonically with the increase in applied load in both dry wear and corrosive wear. As for the environmental effect, the wear rate in 3.5 pct NaCl aqueous solution is larger than that in laboratory air at every applied load. In MMCs, such an effect is less significant for higher Al_2O_3 particulate volume fractions and more significant for higher applied loads. Comparing the curves for dry wear and corrosive wear of monolithic 6061 Al, the wear rate increases linearly with the applied load in dry wear, whereas the curves for corrosive wear level off (*i.e.*, with reduced slopes) at higher applied loads.

The effect of rotational speed on wear rate is illustrated in Figure 4. In general, the wear rate decreases with the increase in rotational speed for both dry wear and corrosive wear. As opposed to the monolithic material, the effect of rotational speed on the wear rate of MMCs is only minor. As for the environmental effect, the wear rate in 3.5 pct NaCl aqueous solution is larger than that in laboratory air at every rotational speed. Because the hydrated aluminum oxide film on the surface is worn out from abrasion, the exposed nascent-abraded active surface forms a new oxide

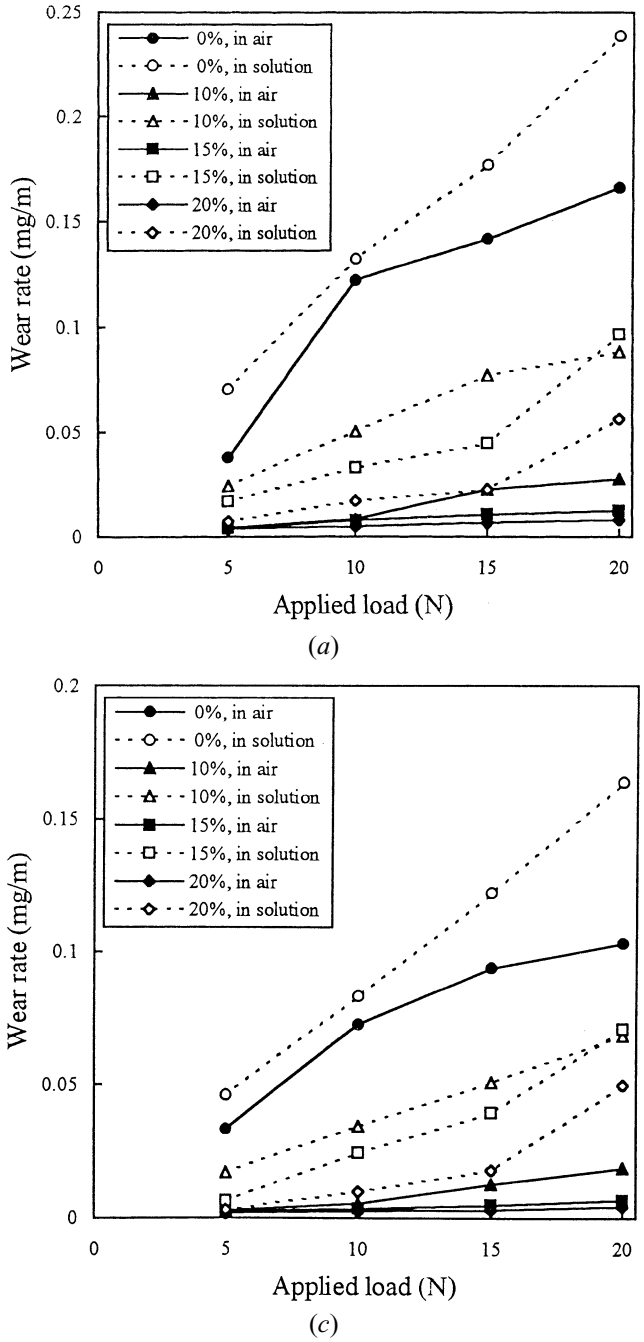

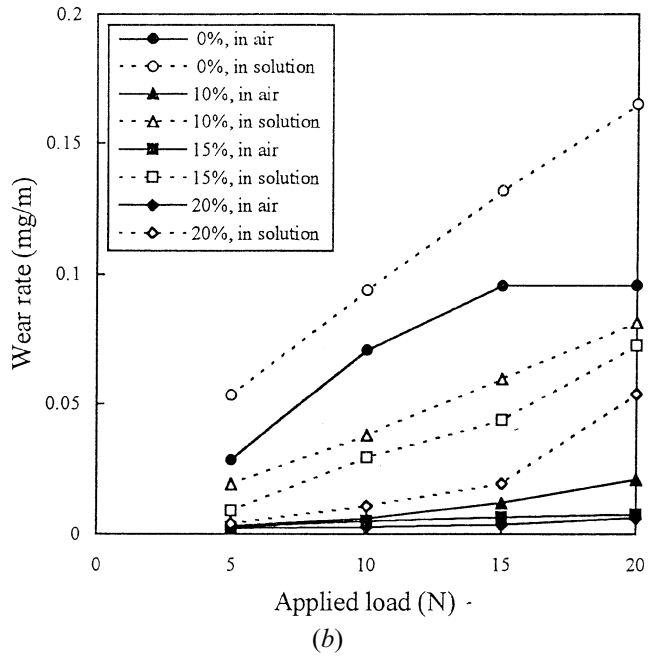

Fig. 3—Effect of the applied load on the wear rate in two environments: (*a*) 100 rpm, (*b*) 300 rpm, and (*c*) 500 rpm.

film, which is subsequently removed again. This process is repeated numerously, resulting in an elevated wear rate. In dry wear, the wear rates for the MMCs are much lower than for the monolithic 6061 Al. However, no significant difference exists between the dry wear rates of the MMCs regardless of the volume fraction of Al_2O_3 particles, particularly at a low applied load (*e.g.*, 5 N), as shown in Figure 4(a). The effect of the particle amount on dry wear resistance becomes more significant for higher applied loads, as shown in Figures 4(c) and (d). Unlike the results in dry wear, the effect of Al_2O_3 volume fractions on corrosive wear rate is rather significant, as indicated by the dashed lines in Figure 4. This might be attributed to the smaller area of metallic surface exposed to the corrosive environment for an increasing amount of Al_2O_3 particulate addition.

The significant reduction in the dry wear rate due to the introduction of reinforcing particles in 6061 Al matrix is not surprising. The fact that MMCs suffer from higher weight loss than the base alloy in corrosion is also expected according to the reported data in the literature.[23,24,30] It is however worth noting that the effect of reinforcement particles on the wear-corrosion resistance turns out to be positive, as indicated by the dashed lines in Figures 3 and 4. Similar results were obtained for SiC_p/Al MMCs.[18] This seems to be contrary to the observation in erosion-corrosion tests,[20,21] attributable to the difference in the mechanisms of erosion corrosion and sliding wear corrosion. For in-

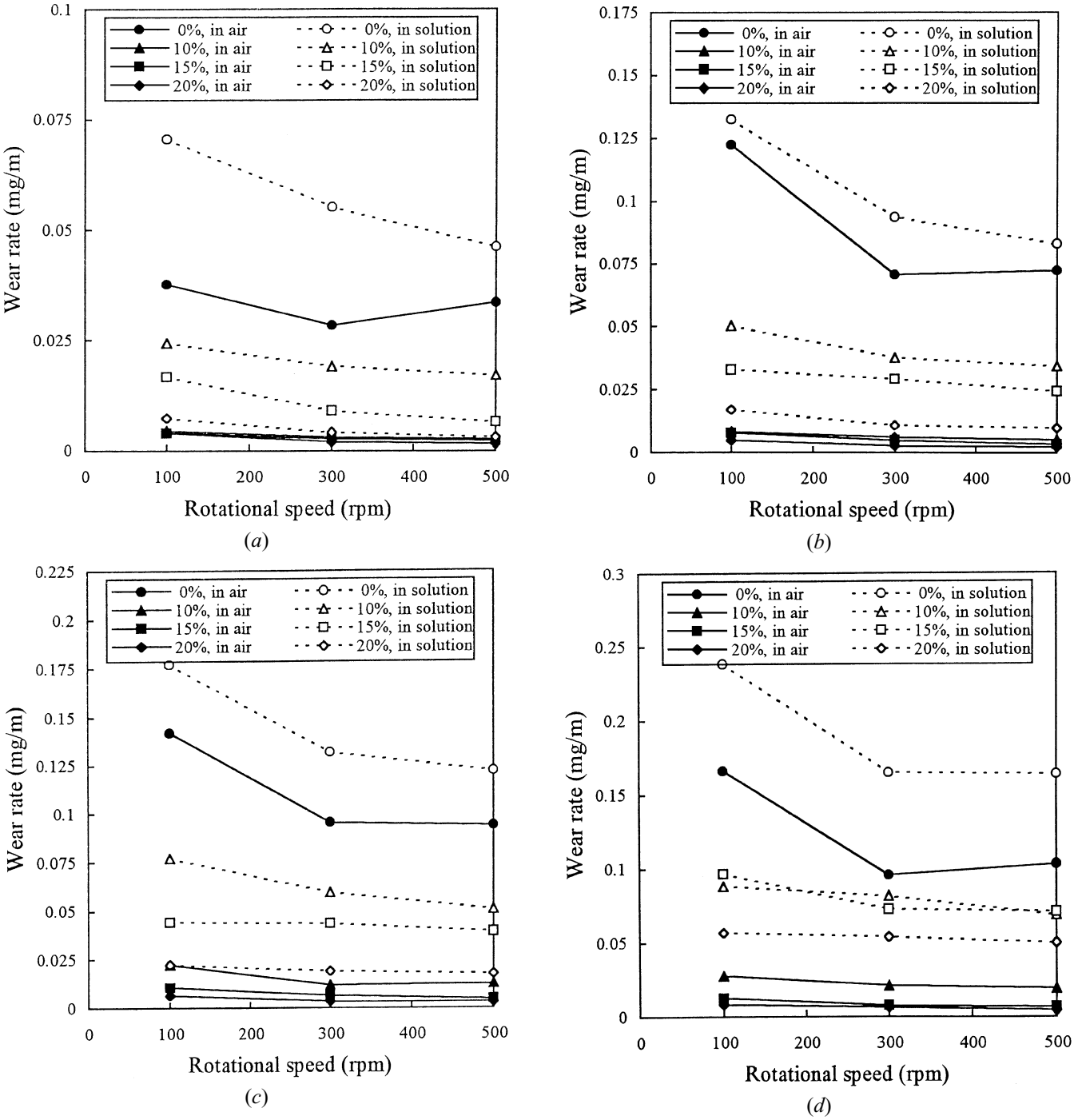

Fig. 4—Effect of the rotational speed on the wear rate in two environments. Applied load: (*a*) 5 N, (*b*) 10 N, (*c*) 15 N, and (*d*) 20 N.

stance, there is no impact force in sliding wear corrosion. The impacts of sand particles in the electrolyte during erosion corrosion will result in rapid formation of pits and craters on the surface.[20] It has been reported that a solid particle erosion (without corrosion) rate for Al-based MMCs is higher than that for their respective matrix alloys.[25–28] Due to the lack of ductility and matrix constraint[26] and the reduction in fracture energy[21] caused by reinforcing particles in the MMCs, the erosion rates increase with the increase in reinforcement additions. In general, it can be postulated that the incorporation of particles in the matrix will diminish the resistance to erosion, corrosion, and erosion corrosion, while increasing the resistance to sliding wear and wear corrosion.

B. *The Effect of Wear on Corrosion Behaviors*

Figure 5 shows the effect of applied load on the corrosion potentials in wear corrosion for monolithic 6061 Al and the MMCs with different volume fractions of reinforcement. For every Al_2O_3 volume fraction, it is found that the corrosion potential tends to be more active as the applied

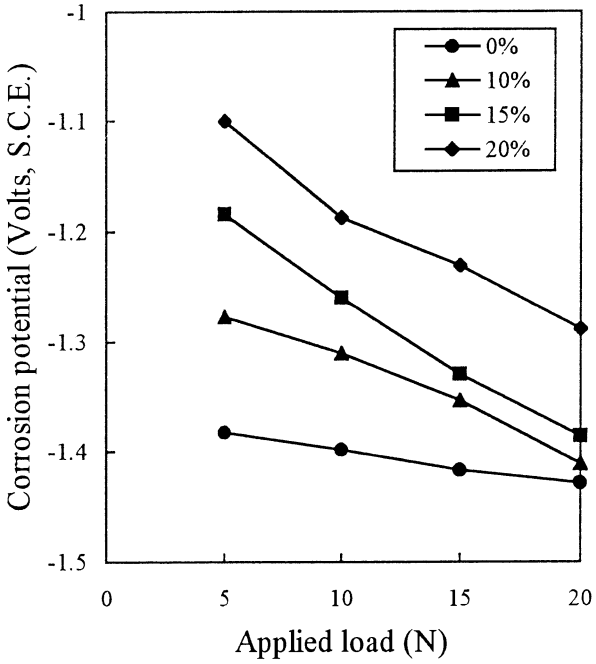

Fig. 5—Effect of the applied load on corrosion potential (rotational speed: 300 rpm).

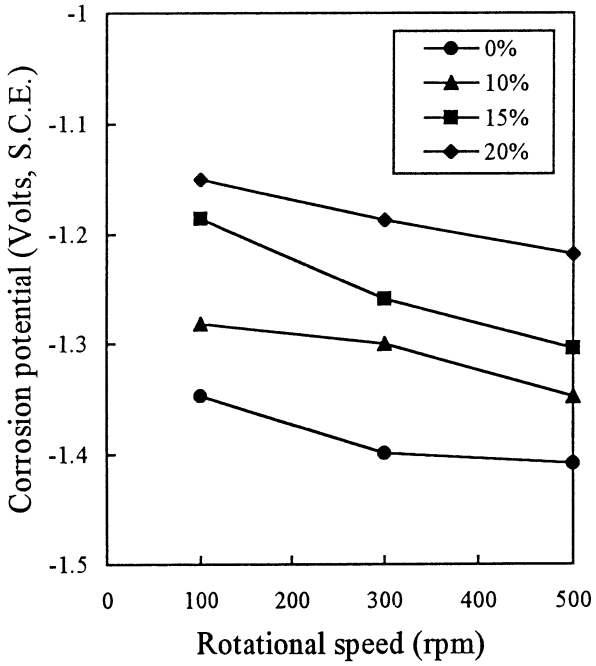

Fig. 6—Effect of the rotational speed on corrosion potential (applied load: 10 N).

load increases. This is because the higher the applied load is, the more fresh and activated the area exposed to the corrosive solution will be. It has also been observed that the corrosion potential becomes more noble if the Al_2O_3 reinforcement amount is increased. Because the particles act as load-bearing elements, as indicated by Alpas and Zhang,[3] the wear rate of the matrix material is reduced due to the increased volume fraction of reinforcement. This imparts in the less exposed fresh surface of the metallic matrix, thus resulting in a more noble corrosion potential.

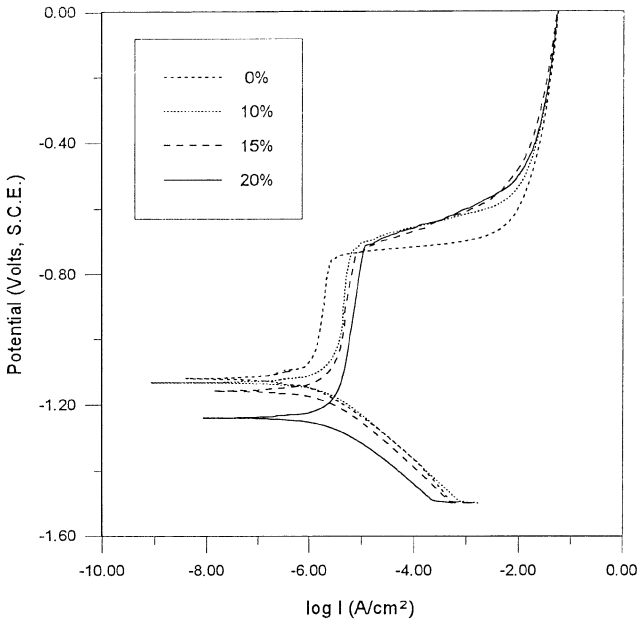

Fig. 7—Potentiodynamic polarization curves of corrosion in a 3.5 pct NaCl solution open to air.

Comparing the slopes of the curves in Figure 5, it is found that the effect of applied load on the corrosion potential is only minor for the monolithic 6061 Al, possibly due to its poor wear resistance. Since most of the active fresh surface of the monolithic 6061 Al has been exposed at the low applied load, 5 N, the increase in the fresh surface by a further increase in the load is very limited. Accordingly, the decrease in corrosion potential with the increased applied load is not significant for the monolithic 6061 Al.

Figure 6 illustrates the effect of rotational speed on corrosion potential. As expected, the corrosion potential shifts to the active side for a higher rotaional speed as a consequence of the shorter time available for repairing the abraded oxide film.

The polarization behavior of the materials with and without wear was then studied. Potentiodynamic polarization curves were generated for corrosion (without wear) in quiescent 3.5 pct NaCl solution. The MMCs with different volume fractions of reinforcement were polarized from −1.5 to 0 V (SCE) with a scan rate of 1 mV/s. As shown in Figure 7, the polarizarion curves for monolithic Al and the MMCs are similar in shape, but different in corrosion potential and passive current density. Each curve shows a passive region. A stable passive film exists at the corrosion potential since no active/passive peak is observed. The MMC with a higher volume fraction of reinforcement results in a more active corrosion potential and a higher passive current density. Similar results for corrosion potential were observed in Sun *et al.*[9] study of SiC_p/Al MMCs in open-to-air tests in 3.5 pct NaCl solution, a consequence of localized corrosion occuring at the reinforcement/matrix interface. Pre-existing defects due to incomplete interfacial cohesion between the matrix and reinforcement allowed easier achievement of the local chemistry required to retard repassivation and enhance localized attack.[12] The likely discontinuity in the surface oxide film due to the changed substrate structure would facilitate the passage of chloride ions to the metal in the NaCl solution. With the interface

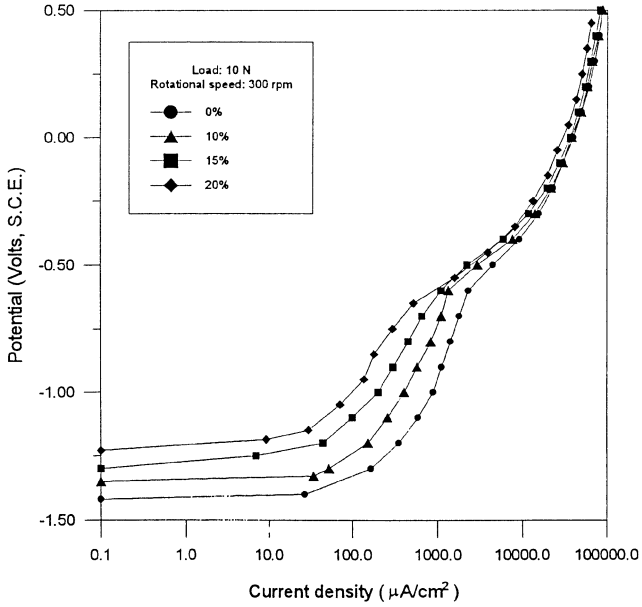

Fig. 8—Potentiostatic anodic polarization curves in wear corrosion.

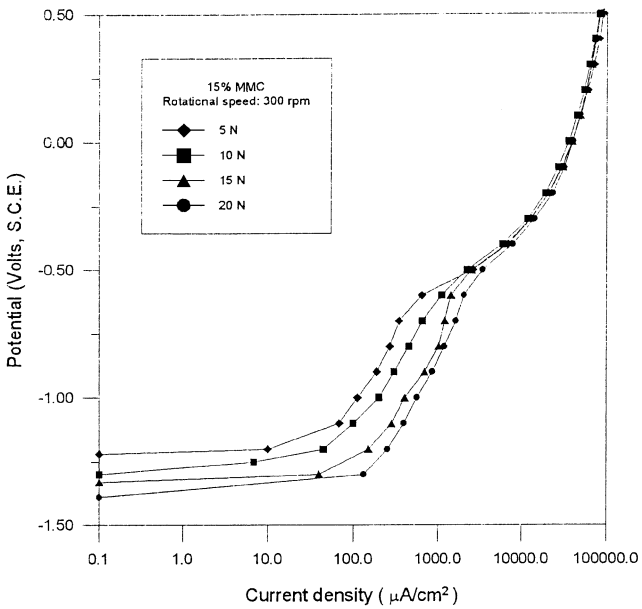

Fig. 9—Effect of the applied load on the potentiostatic polarization curves in wear corrosion.

as a preferential site of corrosion, the corrosion potential shifts to the active side as the volume fraction of the reinforcement is increased.

As shown in Figure 7, the monolithic 6061 Al has about the same pitting potential as the MMCs, suggesting that the introduction of the reinforcement does not significantly affect the susceptibility of the 6061 alloy to pitting—the local break down of the film. Although more intermetallic phases form in the composite than in the monolithic alloy under equivalent conditions of preparation and processing, and hence the composite has more pit initiation sites, pits on the composites are shallower than they are on the monolithic material.[8] These two factors balance each other out somewhat. The particulate reinforcement has therefore only a minor effect on the susceptibility of 6061 alloy to pitting.

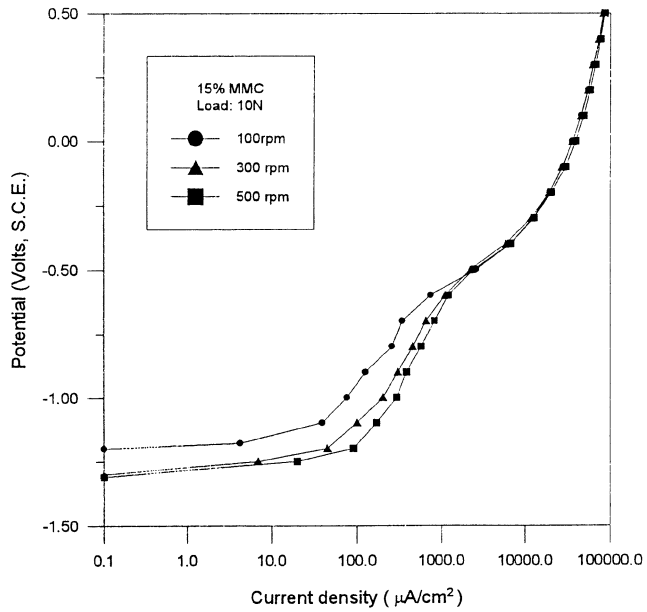

Fig. 10—Effect of the rotational speed on the potentiostatic polarization curves in wear corrosion.

On the other hand, pores are also pit-initiation sites. Since the tested materials had been hot extruded, many of the pores could thus be eliminated and were less important in pitting. This can also be verified by the fact that further increase in the volume fraction of the reinforcement has almost no effect on the pitting potential, as indicated by Figure 7. Similar results were observed for SiC additions.[7] It was found that the introduction of the reinforcement did not substantially affect pitting attack on some Al alloys.[5,7,8] For potentials exceeding the pitting potential, the monolithic Al has the highest current density compared to the MMCs at a given potential, while the current densities for the MMCs are of about the same value.

Figures 8 through 10 present the potentiostatic anodic polarization curves in wear corrosion for different volume fractions of reinforcement, under different applied loads and at different rotational speeds. Comparing Figures 7 and 8, the shape of the polarization curve for wear corrosion is significantly different from that for corrosion. In particular, the passive region appearing in Figure 7 no longer exists in wear corrosion, as shown in Figure 8. The curves in Figures 8 through 10 are similar in shape. As opposed to the results for corrosion shown in Figure 7, the corrosion potential in wear corrosion shifts to the noble side and the current density for an applied potential decreases with the increase in Al_2O_3 volume fraction. In other words, although the incorporation of reinforcement is detrimental to pure corrosion, its effect on wear corrosion is favorable. On the other hand, it was observed that the current density for an applied potential increases with the applied load and rotational speed, as indicated by Figures 9 and 10, respectively. This is again due to the more worn-out passive film of a higher applied load and rotational speed.

C. *Surface Morphologies*

Figures 11 and 12 show the scanning electron micrographs of the wear-corroded surfaces of (a) monolithic 6061

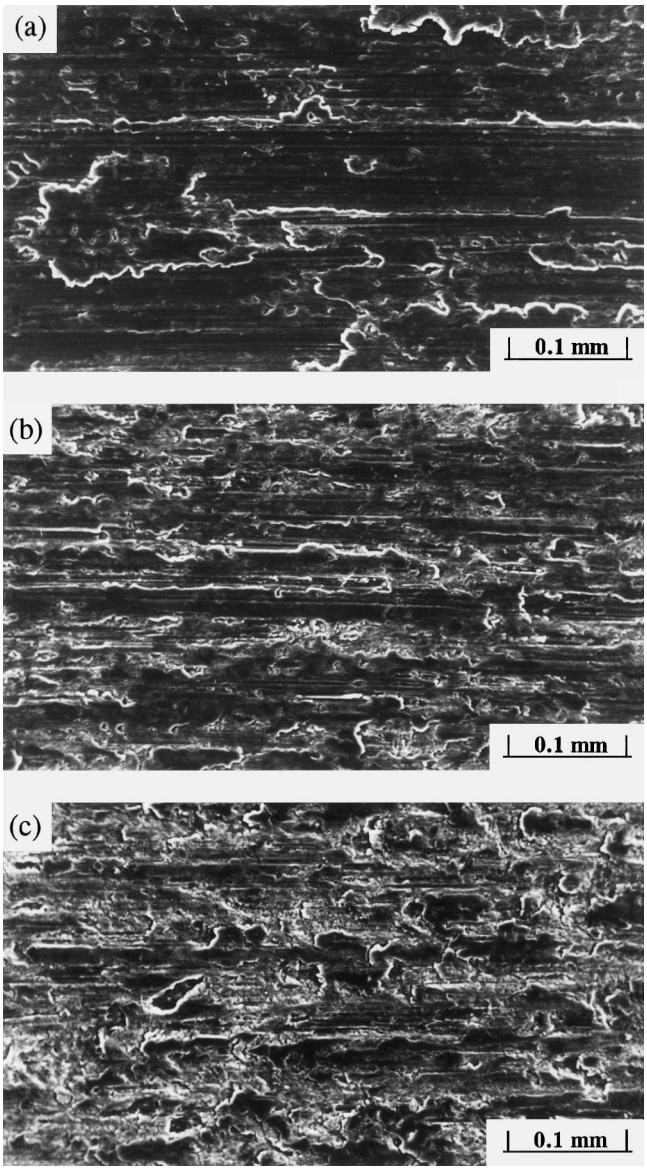

Fig. 11—Surface morphologies after wear corrosion for (*a*) 6061 Al, (*b*) 10-Al_2O_3/Al, and (*c*) 15-Al_2O_3/Al (applied load = 5 N, rotational speed = 300 rpm).

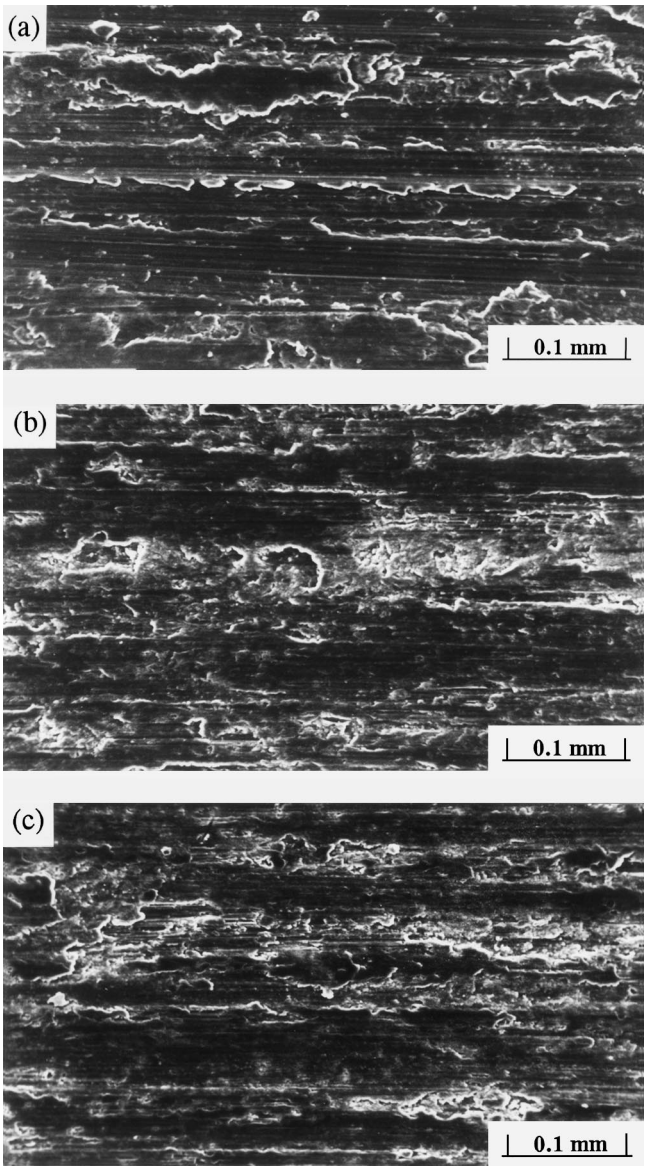

Fig. 12—Surface morphologies after wear corrosion for (*a*) 6061 Al, (*b*) 10-Al_2O_3/Al, and (*c*) 15-Al_2O_3/Al (applied load = 15 N, rotational speed = 300 rpm).

Al, (b) 10-Al_2O_3/Al, and (c) 15-Al_2O_3/Al in 3.5 pct NaCl solution. The rotational speed was 300 rpm, and the applied loads were 5 and 15 N for Figures 11 and 12, respectively. As shown in Figures 11(a) and 12(a), the wear tracks in monolithic 6061 Al have a plough-shaped appearance with materials extruded at the sides of wear tracks. The wear-corroded surface is characterized by fairly long continuous grooves and plastic deformation, while very little wear debris is observed. Most of the corrosion products have been removed by abrasion. As for MMCs, due to the preferential corrosion at the reinforcement/matrix interface, Al_2O_3 particles stand in relief to the matrix. After the passive film on the matrix is abraded, the matrix fails to support the particles. The particles consequently flake off, leaving craters on the surface, as shown in Figures 11(b) and (c) and 12(b) and (c). Pulverization or fragmentation can also be found at the bottom of the flaked areas. The surfaces of the MMCs are relatively rougher than that of monolithic 6061 Al. Comparing Figures 11(a) and (b), the monolithic 6061 has suffered more extensive plastic deformation. In addition to plastic grooving and flaking, voids are evident in the MMCs, as shown in Figure 11(b). This might be due to the plastic deformation of the near-surface region causing locally isolated void formation around the particles.[29] The increase in the volume fraction of reinforcement reduces the extent of plastic deformation in the matrix, as shown in Figure 11(c). Extensive plastic flow is not apparent in the 15-Al_2O_3/Al, while evidence for the presence of microcracks is presented in Figure 11(c). These cracks are more or less perpendicular to the sliding direction.

It is noted that the spatial distribution of the particles may have a significant effect on the wear-corrosion behavior. As illustrated in Figure 1, the micrographs of the tested MMCs show aggregates of particles. The aggregates may

result in easier pullout or dislodging compared to a uniform distribution. Characterization of the uniformity of distributions can be done using standard quantitative metallographic methods. The effect of particle distribution on wear corrosion would be an interesting subject for future research.

IV. CONCLUSIONS

1. In wear corrosion, material degradation is accelerated by wear due to the exposure of fresh active metals by the removal of passive films or corrosion products on the surface.
2. The wear rate in 3.5 wt pct NaCl aqueous solution is larger than that in laboratory air at every applied load and rotational speed. In MMCs, such an effect is less significant for higher Al_2O_3 particulate volume fractions and more significant for higher applied loads.
3. As opposed to the monolithic material, the effect of rotational speed on the wear rate of MMCs is only minor.
4. The incorporation of Al_2O_3 reinforcement improves the wear resistance of 6061 Al. However, the effect of the volume fraction of reinforcement on wear rate is only minor in dry wear, while it is significant in the case of wear corrosion.
5. In wear corrosion, the corrosion potential shifts to the active side and the current density for an applied potential increases with the decrease in Al_2O_3 volume fraction of the materials, with an increase in applied load and rotational speed.
6. Although the incorporation of reinforcement is detrimental to pure corrosion, its influence on wear corrosion is favorable.

REFERENCES

1. F.M. Hosking, F.F. Partillo, R. Wunderlin, and R. Mehrabian: *J. Mater. Sci.*, 1982, vol. 17, pp. 477-98.
2. P.K. Rohatgi, R. Asshana, and S. Das: *Int. Met. Rev.*, 1986, vol. 31 (3), pp. 115-38.
3. A.T. Alpas and J. Zhang: *Wear*, 1992, vol. 155, pp. 83-104.
4. K.D. Lore and J.S. Wolf: *Proc. Meeting of the Electrochemical Society*, Denver, CO, Oct. 1981, Extended Abstract 154.
5. D.M. Aylor and P.J. Moran: *J. Electrochem. Soc.*, 1985, vol. 132, p. 1277.
6. R.B. Bhagat, M.F. Amateau, J.C. Conway, Jr., J.M. Paulick, J.M. Chisholm, J.M. Parnell, and D.G. Seidensticker: *J. Compos. Mater.*, 1989, vol. 23, p. 961.
7. P.P. Trzaskoma, E. Mccafferty, and C.R. Crowe: *J. Electrochem. Soc.*, 1983, vol. 130, pp. 1804-09.
8. P.P. Trzaskoma: *Corrosion*, 1990, vol. 46, pp. 402-09.
9. H. Sun, E.Y. Koo, and H.G. Wheat: *Corrosion*, 1991, vol. 47 (10), pp. 741-53.
10. A.J. Griffiths and A. Turnbull: *Corr. Sci.*, 1994, vol. 36 (1), pp. 23-35.
11. S.L. Coleman, V.D. Scott, and B. McEnaney: *J. Mater. Sci.*, 1994, vol. 29, pp. 2826-34.
12. A. Turnbull: *Br. Corr. J.*, 1992, vol. 27 (1), pp. 27-35.
13. R.C. Paciej and V.S. Agarwala: *Corr. Sci.*, 1988, vol. 44 (10), p. 684.
14. I. Iwasaki, S.C. Riemer, and J.N. Orlich: *Wear*, 1985, vol. 103, pp. 253-67.
15. E.I. Meletis, C.A. Gibbs, and K. Lian: *Dental Mater.*, 1989, vol. 5 (6), pp. 411-14.
16. R.E.J. Noel and A Ball: *Wear*, 1983, vol. 87, pp. 351-61.
17. S.W. Watson, B.W. Madsen, and S.D. Cramer: *Wear*, 1995, vols. 181–183, pp. 469-75.
18. S.Y. Yu, H. Ishii, and T.H. Chuang: *Metall. Mater. Trans. A*, 1996, vol. 27A, pp. 2653-62.
19. J.L. Ji and J.L. Tang: *Wear*, 1990, vol. 138, pp. 23-32.
20. M. Saxena, O.P. Modi, B.K. Prasad, and A.K. Jha: *Wear*, 1993, vol. 169, pp. 119-24.
21. J.A. Bester and A. Ball: *Wear*, 1993, vols. 162–164, pp. 57-63.
22. A. Saigal and G. Leisk: *Scripta Metall. Mater.*, 1992, vol. 26, pp. 871-76.
23. D.M. Aylor: *Metals Handbook*, 9th ed., ASM INTERNATIONAL, Metals Park, OH, 1987, vol. 13, p. 859.
24. O.P. Modi, M. Saxena, B.K. Prasad, A.H. Yegneswaran, and M.L. Vaidya: *J. Mater. Sci.*, 1992, vol. 27, p. 3897.
25. S. Srinivasan, R.O. Scattergood, and R. Warren: *Metall. Trans. A*, 1988, vol. 19A, pp. 1785-93.
26. K.C. Goretta, W. Wu, J.L. Routbort, and P.K. Rohatgi: *Proc. Congr. Tribology of Composite Materials*, Oak Ridge, TN, May 1–3, 1990, P.K. Rohatgi, C.S. Yust, and P.J. Blau, eds., ASM INTERNATIONAL, Materials Park, OH, 1990, pp. 147-55.
27. I.M. Hutchings and A. Wang: *Proc. Conf. on New Materials and Their Applications*, Warwick, England, Apr. 1990, Institute of Physics Conf. Series, Institute of Physics, Bristol, United Kingdom, 1990, pp. 111-20.
28. S. Wilson and A. Ball: *Advances in Composite Technology*, Composite Materials Series 8, K. Friederich, ed., Elsevier, New York, NY, 1993, pp. 311-66.
29. A. Wang and H.J. Rack: *Mater. Sci. Eng.*, 1991, vol. A147, pp. 211-24.
30. M.S.N. Bhat, M.K. Surappa, and H.V.S. Nayak: *J. Mater. Sci.*, 1991, vol. 26, pp. 4991-96.